

TECHNICAL NOTE

Three-dimensional electrokinetic tweezing: device design, modeling, and control algorithms

Roland Probst¹ and Benjamin Shapiro²

¹ Fischell Department of Bioengineering, University of Maryland, College Park, MD 20742, USA

² Fischell Department of Bioengineering and Institute for Systems Research, 1226 Kim, University of Maryland, College Park, MD 20742, USA

E-mail: rolandp@umd.edu and benshap@umd.edu

Received 24 November 2010

Published 27 January 2011

Online at stacks.iop.org/JMM/21/027004

Abstract

We show how to extend electrokinetic tweezing (which can manipulate any visible particles and has more favorable force scaling than optical actuation enabling manipulation of nanoscale objects to nanoscopic precision) from two-dimensional control to the third dimension (3D). A novel and practical multi-layer device is presented that can create both planar and vertical flow and electric field modes. Feedback control algorithms are developed and demonstrated in realistic simulations to show 3D manipulation of one and two particles independently. The design and control results presented here are the essential next step to go from current 2D manipulation capabilities to an experimental demonstration of nano-precise 3D electrokinetic tweezing in a microfluidic system. Doing so requires integration with vision-based nano-precise 3D particle imaging, a capability that has been shown in the literature and which we are now combining with the 3D actuation and control methods demonstrated here.

 Online supplementary data available from stacks.iop.org/JMM/21/027004/mmedia

(Some figures in this article are in colour only in the electronic version)

Introduction

Vision-based electrokinetic feedback control (figure 1) has allowed simple microfluidic devices to manipulate microscopic and nanoscopic objects on chip [1–5]. Electrokinetic (EK) manipulation, which includes electrophoretic [6] and electroosmotic [7, 8] actuation, does not require lasers and does not rely on the dielectric properties of the particles to be manipulated. It differs from dielectrophoretic (DEP) [9–11] actuation, which exploits spatial non-uniformity and temporal frequency (alternating current) of the applied electric fields to create forces on dielectric particles in that even a spatially constant and steady (direct current) electric field will create EK forces. DEP actuation has been used to trap [12–14], sort [15, 16], and

move particles by sequentially trapping them in adjacent traps [17]. EK tweezing allows control of essentially any visible objects [4, 5, 18]. It has enabled on-chip individual manipulation of one and multiple cells [4], including the steering and trapping of live swimming cells [18]. The favorable scaling of electroosmotic (EO) actuation (drag forces scale with particle size [19] rather than with particle volume as do optical and DEP forces [20]) has further allowed control of nanoscopic particles to tens of nanometers precision [5, 21], the best reported precision to date of any method. EK manipulation may also be able to control the orientation of objects in addition to their positions [22] by modulating the shear around them to cause controlled object rotations. However, all of these prior results have been restricted to control in two spatial dimensions only.

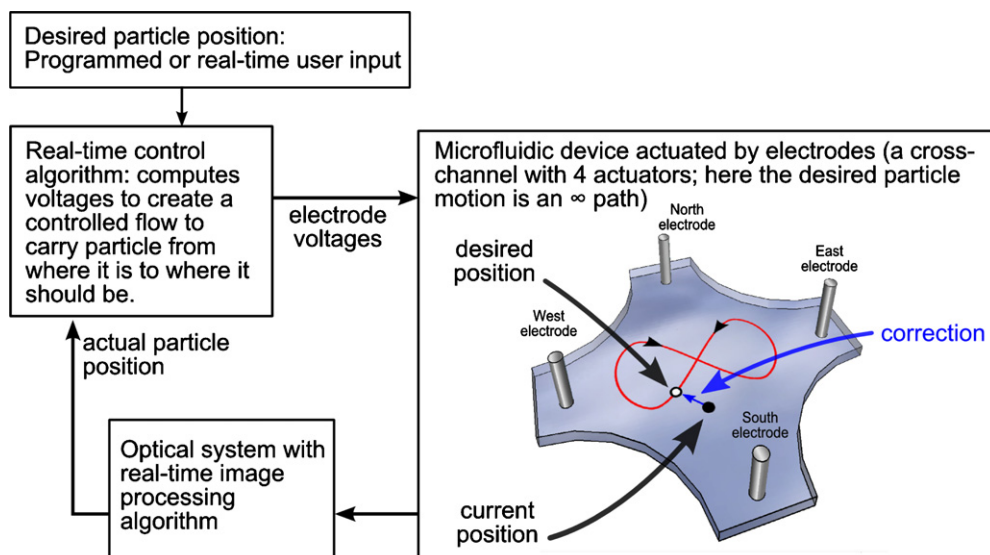


Figure 1. Feedback control manipulation approach for a single particle. A micro-fluidic device with EK (EO or electrophoretic) actuation is observed by a vision system that informs the control algorithm of the current particle position. The control algorithm compares this actual position (black dot) against the desired position (open circle) and finds the actuator voltages that will create a velocity, at the particles location, to steer the particle from where it is to where it should be. The process repeats continuously to steer the particle along its desired path. Device fabrication, vision sensing, and control design for implementing such a system is covered in detail in [4, 18]; the latter reference includes both a detailed protocol as well as sensing and control software to realize the feedback manipulation.

Here we present a device design, along with the associated modeling and control, which can extend EK trapping and steering capabilities to the third dimension. The modeling, algorithm, and simulation results we present here are a prerequisite to subsequent experimental demonstrations, as has been the case for all our prior theory developments [22–26] that subsequently led to experimental demonstrations for control of one and multiple cells [4, 18], swimming bacteria [18], and EK tweezing of single quantum dots to tens of nanometers precision [5, 27].

As in [28–30], the concept is to cross channels one above the other to enable vertical force components. Modeling of the electrophoretic and EO physics, that then informs advanced control design, enables trapping and steering of both neutral and charged particles, to high precision, across a wide working region. Our design incorporates all the lessons learned from prior experimental work. It places the electrodes far away from the control region to prevent the generation of bubbles by electrolysis from interrupting the control; it has a flat and clear control region to provide easy and distortion free optical access as will be needed for horizontal and vertical position sensing [31, 32]; and its layered structure is both straightforward to fabricate and creates significant electrophoretic and EO vertical force components. For this new device, we state a 3D first-principles physical model for EP forces and EO flows based on our prior experimentally validated models [4, 23], and we then develop algorithms for and demonstrate 3D control of one and two particles in simulations.

We first briefly summarize how EK tweezers work in two spatial dimensions [4, 18, 23] before showing how to extend the method to work in the third dimension. As shown in figure 1, a micro-fluidic device, a vision system (microscope, camera, and particle detection software), and a

control algorithm are connected in a feedback loop. The vision system identifies the location of each particle in real time; the control algorithm then compares the current position of a target particle with its desired position. If the two positions differ then the actuating electrodes create the right EK velocity (at the particle's location) to move it from where it is toward where it should be. This velocity can either be created by an electric field to move a charged particle relative to the buffer (EP actuation), or by an EO actuation of the flow that will carry a neutral particle along, or by a combination of both. The whole feedback loop repeats at each time step to continually move any target particle from its actual position closer to its desired location, thus either trapping it (continually putting it back to a stationary desired location) or steering it (continually moving it to a new desired location). This process is robust to device imperfections and flow uncertainties—so long as the control knows how to actuate the electrodes to move the particle from where it is to *closer* to where it should be; it decreases the displacement error at each time step and quickly drives the particle to its target location, with up to 46 nm precision [5].

Device design

Instead of one planar layer [4, 18], the device for 3D control consists of three layers which can be fabricated by replica molding of PDMS to create multi-layered PDMS devices as described in Jo *et al* [33] and Zhang *et al* [34]. As shown in figure 2, the top and bottom layers contain the micro channels and the middle layer has a through hole which connects them. In this middle intersection the flow coming from a top channel can move into a lower channel and vice versa. Therefore, any object located in the intersection can experience a sink or lift force if the actuation is applied from a top to a bottom electrode

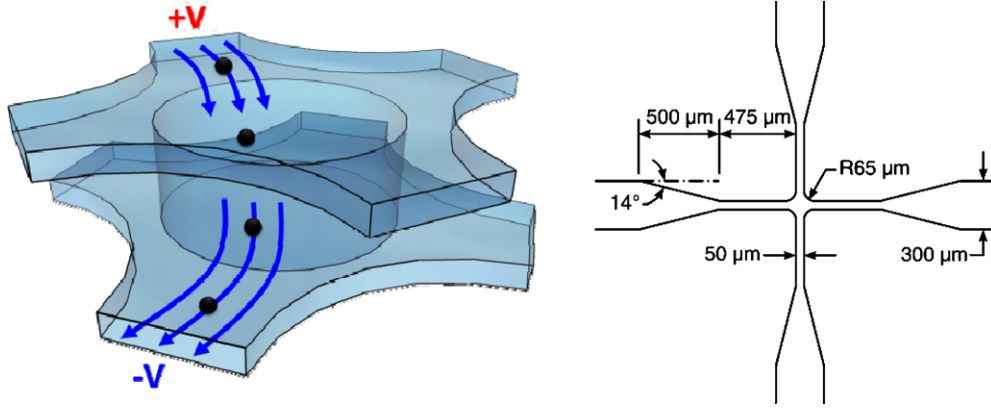


Figure 2. (a) Device design for 3D EK tweezing. By applying voltages between channels in the top and bottom layers, an up or down electrophoretic force or EO flow component can be created at the particles location, in addition to the usual horizontal actuation. (b) Fabrication of the device can be achieved by overlaying two optimized planar EK control devices above and below a PDMS layer with a hole. Example dimensions are shown; the channels are 50 μm wide, 10 μm high and intersect at a 130 μm diameter control region. The middle layer could be 30 μm thick with a 60 μm diameter through hole.

or vice versa. This can move a particle in the third dimension using either electrophoretic or EO actuation.

Governing equations

We first consider the simpler EP case only: the physics of 3D electrophoretic particle actuation in a quiescent fluid (no EO flow yet). As is the case in planar EP control experiments, when a small charged particle sees an electro-static force it quickly achieves an equilibrium electrophoretic velocity in the direction of the applied electric field at its location [23, 35, 36]. The electrophoretic velocity of the particle in an electrolyte can be characterized by its zeta potential ζ_p and is given by the Helmolz–Smoluchowski relation [19]:

$$\vec{v}_{ep} = \mu_{ep} \vec{E} = \frac{\varepsilon_0 \varepsilon_r \zeta_p}{\eta} \vec{E}, \quad (1)$$

where μ_{ep} is the electrophoretic mobility of the particle, η is the dynamic viscosity of the liquid, ε_r is the relative dielectric constant of the liquid and ε_0 is the dielectric constant in vacuum. The 3D electric field $\vec{E} = -\nabla\Phi$ we create in the device is described by Laplace’s equation subject to boundary conditions set by the voltages we apply at the eight electrodes. Since Laplace’s equation is linear we can write the net actuated electric field as a superposition of the fields produced by each electrode alone:

$$E(x, y, z, t) = - \sum_{i=1}^8 \nabla\Phi_i(x, y, z) V_i(t), \quad (2)$$

where Φ_i denotes the electric potential when electrode i is turned on to a unit voltage ($V_i = 1$) and all the other electrodes are set to zero. The dynamics for a charged particle anywhere in the control chamber is now given by

$$\begin{aligned} (\dot{x}, \dot{y}, \dot{z}) &= \vec{v}_{ep} + \vec{w} \\ &= -\mu_{EP} \sum_{i=1}^8 \nabla\Phi_i(x, y, z) V_i(t) + \vec{w}(t) \\ &= [A_{ep}(x, y, z)] \vec{V}(t) + \vec{w}(t). \end{aligned} \quad (3)$$

This means that the particle’s next location is determined by the applied 3D electric field at its current (x, y, z) location and by thermal Brownian noise [19], which is written as $d\vec{w} = \vec{n}\sqrt{kTdt}/6\pi\eta a$ for a spherical particle of radius a where k is the Boltzman constant, T is the ambient temperature, η is the dynamic viscosity of the liquid as before, \vec{n} is a Gaussian random vector of zero mean and unit variance, and dt is the differential time interval [37]. The matrix A_{ep} summarizes the shape of the electric gradients created by all the electrodes and $\vec{V} = [V_1, V_2, \dots, V_8]$ is the vector of controlled electrode voltages. We note that during experimental control of both micro- and nano-scale particles [4, 5, 38], for our modest electric field strengths ($|\vec{E}| \sim 50 \text{ V cm}^{-1}$) and $\sim 30 \text{ Hz}$ temporal variations of the electric fields we apply, DEP effects are not observed.

The physics for EO actuation of neutral particles is more complex but highlights the same essential features; the particle motion is linear in the applied voltages but the created velocity, including up and down actuations, varies nonlinearly with the particles location. In EO actuation, each solid/liquid interface in the device develops a thin electric double layer that moves under the applied electric field and drags the adjacent fluid along by viscous forces [19]. Thus the flow at each solid interface of the device follows the local electric field:

$$\vec{v}_{eo}|_I = \mu_{eo} \vec{E}|_I = \frac{\varepsilon_0 \varepsilon \xi_I}{4\pi\eta} \vec{E}|_I, \quad (4)$$

where v_{eo} is the EO fluid velocity at the liquid/solid interfaces (denoted by $|_I$). The Reynolds number in our devices is small ($Re \sim 5 \times 10^{-5}$) and so in the interior of the device the fluid flow is accurately described by the Stokes equations [19]:

$$\nabla \cdot \vec{v}_{eo} = 0, \quad \eta \nabla^2 \vec{v}_{eo} = \nabla p. \quad (5)$$

Here p is the pressure and the two equations state the conservation of mass and momentum. Equation (4) above acts as the boundary condition for these Stokes equations where the electric field is as given previously in equation (2). Since both the electric field and the Stokes equations are linear, we can

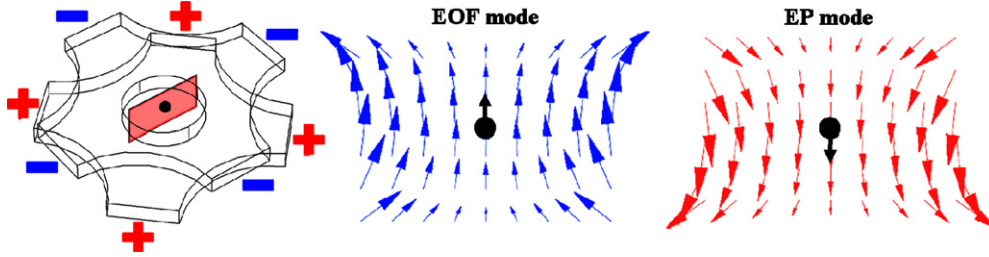


Figure 3. Sample EO and EP vertical actuation velocities in the marked pink vertical plane. The created velocities are shown at each location in the plane and in particular for the black particle in the center. The two velocities differ in sign since, for the values in table 1, the particle acquires negative surface charge; otherwise, EO and EP velocities are similar but not identical. Since only a non-zero vertical component is required for effective 3D control, particles can be controlled even when they are far from the center (as shown in figures 4, 5 and 6).

still write the final fluid velocity as a superposition of the EO velocities due to each electrode

$$\vec{v}_{eo} = \sum_{i=1}^8 \vec{v}_{eo}^i(x, y, z) V_i(t), \quad (6)$$

where $\vec{v}_{eo}^i(x, y, z)$ is the 3D EO flow velocity caused by turning on electrode i to a unit voltage and setting all the other voltages to zero. The dynamics of a neutral particle anywhere in the control region is therefore

$$\begin{aligned} (\dot{x}, \dot{y}, \dot{z}) &= \vec{v}_{eo} + \vec{w} \\ &= \sum_{i=1}^8 \vec{v}_{eo}^i(x, y, z) V_i(t) + \vec{w}(t) \\ &= [A_{eo}(x, y, z)] \vec{V}(t) + \vec{w}(t). \end{aligned} \quad (7)$$

The motion of a charged particle in the presence of EO flow is the sum of EP and EO contributions:

$$\begin{aligned} (\dot{x}, \dot{y}, \dot{z}) &= \sum_{i=1}^n [\vec{v}_{eo}^i(x, y, z) - \mu_{EP} \nabla \Phi_i(x, y, z)] V_i(t) + \vec{w}(t) \\ &= [A_{ek}(x, y, z)] \vec{V}(t) + \vec{w}(t). \end{aligned} \quad (8)$$

Equations (3), (7), or (8) are the mapping, for charged or neutral particles, with or without EO flow, from electrode actuators V_i to the resulting particle motion. To achieve precision manipulation there is no need for this mapping to be perfectly accurate; it just has to be sufficient to tell the control algorithm how to move the particle from where it is *toward* where it should be so as to shrink the error at each time step. Figure 3 illustrates a sample EO (\vec{v}_{eo}) and electrophoretic (\vec{v}_{ep}) vertical actuation mode for the case when all bottom electrodes are turned on positive and all the top electrodes are negative. The simulation parameters considered here have been chosen to match the surface chemistry conditions we have in our current planar PDMS devices [4, 5, 18, 38], and the electric fields we commonly use (up to ~ 10 V on each electrode). Side-by-side, at each location, we show the vertical velocity a particle would experience at that location.

Control

Control design for 3D manipulation is based on our prior nonlinear control design for 2D multi-particle control [4, 23] with the new feature that we now consider an additional actuation degree of freedom per particle to account for motion

Table 1. Values of parameters used for simulations.

Parameter	Value	Description
η	1×10^{-3} Pa s	Viscosity
ρ	1×10^3 kg m $^{-3}$	Density
σ	0.01 S m $^{-1}$	Electric conductivity, water
ϵ_r	78.3	Relative permeability, water
ζ_{PDMS}	-50 mV	Zeta potential (PDMS)
ζ_{particle}	36.2 mV	Zeta potential (QD) source: Hoshino <i>et al</i> [39]
E_{max}	~ 5700 V m $^{-1}$	Electric field (max)
∇E_{max}	4.9×10^8 V m $^{-2}$	Electric field gradient (max)

in the third dimension. For the location of each particle, we have a linear map (according to either equations (1) and (2) for EP actuation; or equation (6) for EO actuation; or the sum of both) from the electrode voltages to the created 3D velocities at the particle locations. As in [4, 23], this map is inverted by a pseudo-inverse (least-squares) method to find the voltages that will best achieve the desired correcting particle velocities and these are applied at each time step [4, 18, 23]. This leads to the control law

$$\vec{V} = -kA^\dagger(\vec{r}) \vec{v}_{\text{req}}, \quad (9)$$

where \vec{V} is the control voltage vector, \vec{v}_{req} is the desired particle velocity vector, $\vec{r} = (x, y, z)$ is the position vector, k is a positive scalar and $A^\dagger = (A^T A)^{-1} A^T$ is the pseudo inverse of the linear map (according to either equations (3), (7), or (8)). This 3D control algorithm is non-standard; it is linear in the instantaneous mapping from the current particle positions to applied voltages, but it is nonlinear with respect to motion—the least-squares map changes nonlinearly as the particles move [23].

Simulation results are shown next for a single microscopic particle being controlled electroosmotically along a vertical infinity sign (figure 4) and two particles being controlled at once by EP along two circles in orthogonal planes (figure 5).

Control of two 10 nm diameter particles (whose Brownian motion is significant in water) is shown along two orthogonal and self-intersecting circles in figure 6. In this case we further assume that the control algorithm does not accurately know the charge on these particles—it believes their charge is $\pm 50\%$ of the true value. As in our prior work, EK tweezing is not sensitive to such errors because the control always corrects the particles from where they are toward where they should be, and

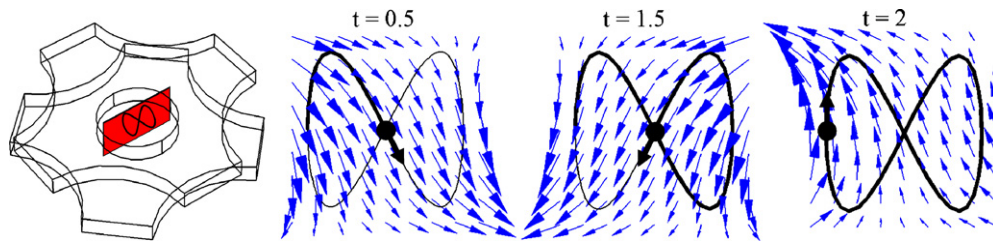


Figure 4. Control of one particle (black dot) on a vertical infinity path by EO actuation. The desired path of the particle is in thin black, the achieved path is in thick black, and the arrows show the EO velocity field at each time step. See movie 1 in the supplementary data, available at stacks.iop.org/JMM/21/027004/mmedia.

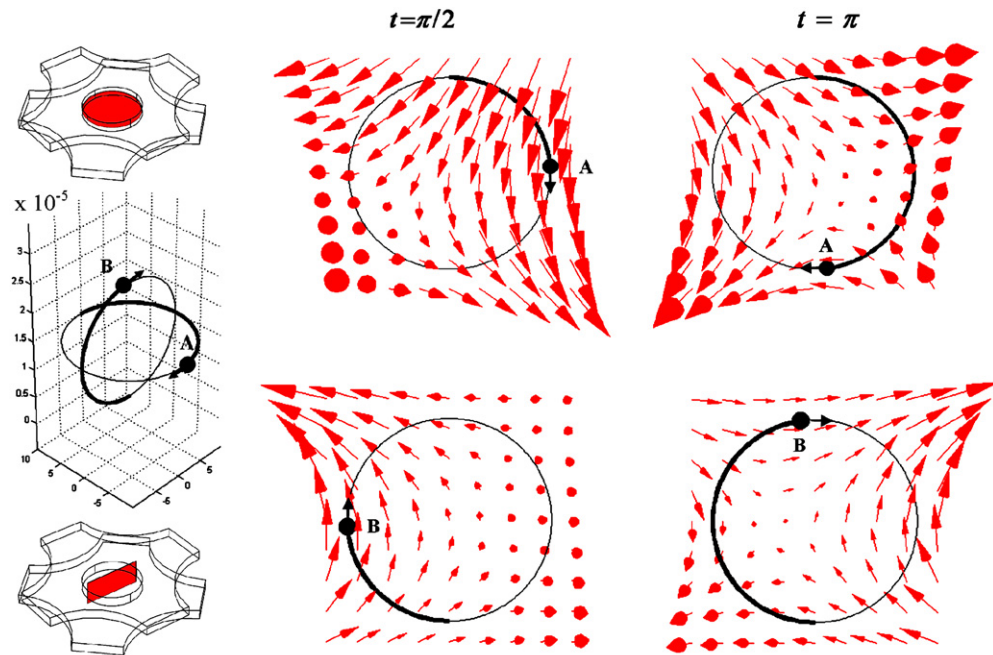


Figure 5. Two particles controlled simultaneously on two orthogonal circular paths. The horizontal and vertical paths are shown at the top and the bottom of the figure respectively. The desired path of the two particles (A) and (B) is in thin black and the achieved path is in thick black. The (red) arrows show the EP velocity field at the two time instants (arrows that appear as round dots show flow coming out of that plane). See movie 2 in the supplementary data, available at stacks.iop.org/JMM/21/027004/mmedia.

it does so successfully even if it has only a partial knowledge of particle properties. In this case manipulation is predicted to be achieved to a precision of $2\ \mu\text{m}$. We have verified that our 3D control scheme works in simulations for either positive or negatively charged particles. Further, as done in [4], if needed, during experiments the charge of the particles can be readily estimated offline or online (during control operation) by a Kalman filter [40, 41] which optimally estimates the velocity of the particles moving under the known applied electric fields and thus infers their individual charges.

EK tweezing precision is set by imaging accuracy plus Brownian motion. The control knows the location of the particle as good as the vision system can measure it; between control updates each particle diffuses away until the next control actuation brings it back. Control forces scale with particle radius for EO actuation, and with surface charge for EP actuation, and have proved to be sufficient to effectively actuate even nanoscopic objects. In Ropp *et al* [5] we achieved 2D EO manipulation of single (6 nm diameter) quantum dots to nanoscopic accuracy—we followed a $50\ \mu\text{m}$ long ‘QD’

trajectory with 120 nm average error and then held a desired QD to 45 nm precision. This was done by using subpixel averaging [42] on the diffraction image to measure the location of the center of the QD to much better resolution than the wavelength of light (to 19 nm), and by adding an associating polymer to the water to increase its viscosity and thus decrease QD diffusion between control actions.

In order to extend our nano-precise EK tweezers from two to three dimensions, we must combine the capabilities presented here with nano-precise 3D particle imaging. This type of imaging has recently been demonstrated by Juette and Bewersdorf [43] (for 200 nm fluorescent particles in water). They sensed particle 3D location by combining aspects of CCD camera-based multiplane imaging and a feedback-driven focused laser beam to achieve a depth detection range of $100\ \mu\text{m}$ and localization precision of $\sim 8\ \text{nm}$ lateral and $\sim 27\ \text{nm}$ vertical. McMahon *et al* [44] achieved comparable localization precisions using angled micro mirrors. Using these types of methods, we are working to tighten our vertical sensing accuracy, and to combine it with device fabrication

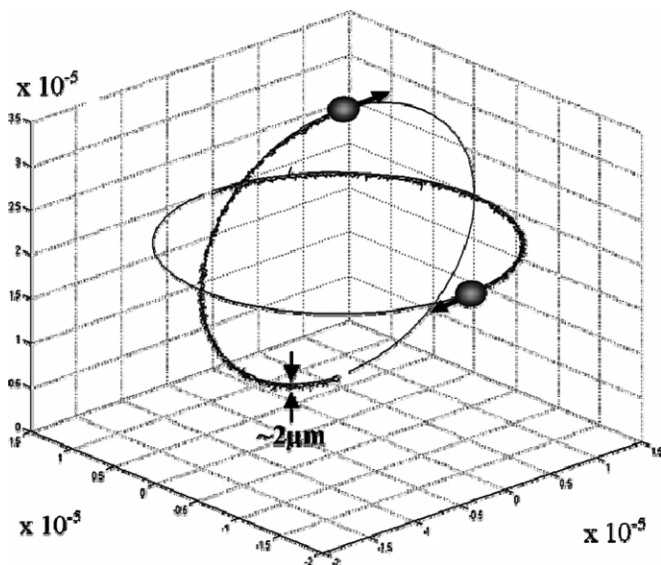


Figure 6. Two nanoparticles (diameter 10 nm) controlled simultaneously in the presence of Brownian motion and a 50% charge uncertainty. See movie 3 in the supplementary data, available at stacks.iop.org/JMM/21/027004/mmedia.

and our control methods above to demonstrate on-chip three-dimensional nano-precise EK tweezing.

Conclusion

We have created a novel and simple device design, developed model-based advanced control algorithms, and shown realistic simulations for 3D EK trapping and steering of single particles. The designed device is based on past EK tweezing systems that have achieved control of one and multiple cells, swimming cells, and single QDs to tens of nanometer precision. It can be fabricated by replica molding of PDMS and its behavior is quantified by the first-principles models presented here. Feedback control algorithms for this device were extended from prior work on multi-particle control and show expected, robust, and high-performance behavior in simulations. Based on these necessary modeling, device design, and control development steps, we are now working to fabricate the devices and improve our imaging in the third dimension to experimentally demonstrate three-dimensional EK tweezing of neutral and charged particles. Extending EK tweezing to the third dimension would enhance the manipulation of biomolecules in lab-on-a-chip settings and could enable precision placement of QDs to the top of raised features, such as high-Q ring resonators.

Acknowledgments

This research was supported in part by DARPA (W31P4Q-0810007), the Institute of Systems Research at the University of Maryland, and by the National Science Foundation (CAREER grant, program managers Maria Burka and Kishan Baheti, grant number ECS0348251).

References

- [1] Armani M, Chaudhary S, Probst R and Shapiro B 2004 Micro flow control particle tweezers *uTAS, Malmo, Sweden* pp 26–30
- [2] Armani M, Chaudhary S, Probst R and Shapiro B 2005 Using feedback control and micro-fluidics to steer individual particles *18th IEEE Int. Conf. on Micro Electro Mechanical Systems (Miami, Florida)* pp 855–8
- [3] Cohen A E 2005 Control of nanoparticles with arbitrary two-dimensional force fields *Phys. Rev. Lett.* **94** 118102
- [4] Armani M, Chaudhary S, Probst R and Shapiro B 2006 Using feedback control and microflows to independently steer multiple particles *J. Microelectromech. Syst.* **15** 945–56
- [5] Ropp C, Probst R, Cummins Z, Kumar R, Berglund A, Raghavan S, Waks E and Shapiro B 2010 Manipulating quantum dots to nanometer precision by control of flow *Nano Lett.* **10** 2525–30
- [6] Barz D P J and Ehrhard P 2005 Model and verification of electrokinetic flow and transport in a micro-electrophoresis device *Lab Chip* **5** 949–58
- [7] Santiago J G 2001 Electroosmotic flows in microchannels with finite inertial and pressure forces *Anal. Chem.* **73** 2353–65
- [8] Laser D J and Santiago J G 2004 A review of micropumps *J. Micromech. Microeng.* **14** R35–64
- [9] Pohl H A 1978 *Dielectrophoresis: The Behavior of Neutral Matter in Nonuniform Electric Fields* (Cambridge: Cambridge University Press)
- [10] Jones T B 2005 *Electromechanics of Particles* (Cambridge: Cambridge University Press)
- [11] Edwards B, Engheta N and Evoy S 2007 Electric tweezers: experimental study of positive dielectrophoresis-based positioning and orientation of a nanorod *J. Appl. Phys.* **102** 024913
- [12] Müller T 1996 Trapping of micrometre and sub-micrometre particles by high-frequency electric fields and hydrodynamic forces *J. Phys. D: Appl. Phys.* **29** 340–9
- [13] Thomas R S, Morgan H and Green N G 2009 Negative DEP traps for single cell immobilisation *Lab Chip* **9** 1534–40
- [14] Chou C-F, Tegenfeldt J O, Bakajin O, Chan S S, Cox E C, Darnton N, Duke T and Austin R H 2002 Electrodeless dielectrophoresis of single- and double-stranded DNA *Biophys. J.* **83** 2170–9
- [15] Hughes M P 2002 Strategies for dielectrophoretic separation in laboratory-on-a-chip systems *Electrophoresis* **23** 2569–82
- [16] Nieuwenhuis J H, Jachimowicz A, Svasek P and Vellekoop M J 2004 High-speed integrated particle sorters based on dielectrophoresis *Sensors (Vienna, Austria)* pp 64–7
- [17] Morgan H *et al* 1997 Large-area travelling-wave dielectrophoresis particle separator *J. Micromech. Microeng.* **7** 65–70
- [18] Probst R, Cummins Z and Shapiro B 2010 Electrokinetic tweezers: living cells manipulation by vision sensing and electrokinetic feedback control *Nature Protoc.* accepted with revisions
- [19] Probstein R F 2003 *Physicochemical Hydrodynamics: An Introduction* (New York: Wiley)
- [20] Dienerowitz M, Mazilu M and Dholakia K 2008 Optical manipulation of nanoparticles: a review *J. Nanophotonics* **2** 021875
- [21] Cohen A E and Moerner W E 2008 Controlling Brownian motion of single protein molecules and single fluorophores in aqueous buffer *Opt. Express* **16** 6941–56
- [22] Mathai P P, Berglund A J, Liddle J A and Shapiro B A 2010 Simultaneous positioning and orientation of a single nanorod by flow control, in preparation
- [23] Chaudhary S and Shapiro B 2006 Arbitrary steering of multiple particles at once in an electroosmotically driven

- microfluidic system *IEEE Trans. Control Syst. Technol.* **14** 669–80
- [24] Walker S and Shapiro B 2005 A control method for steering individual particles inside liquid droplets actuated by electrowetting *Lab Chip* **12** 1404–7
- [25] Walker S W, Shapiro B and Nochetto R H 2009 Electrowetting with contact line pinning: computational modeling and comparisons with experiments *Phys. Fluids* **23** 102103
- [26] Armani M, Chaudhary S, Probst R, Walker S and Shapiro B 2005 Control of micro-fluidic systems: two examples, results and challenges *Int. J. Robust Nonlinear Control* **15** 785–803
- [27] Gorman J and Shapiro B 2010 Feedback control of systems on the micro- and nano-scales: from MEMS to atoms *Microsystems Series* ed S Senturion (New York: Springer)
- [28] Davis L *et al* 2008 Maximum-likelihood position sensing and actively controlled electrokinetic transport for single-molecule trapping *Proc. SPIE* **6862** 68620p
- [29] Probst R and Shapiro B 2008 Micro fluidic device that allows 3 dimensional control of nano and micro particles by electroosmotic flow (EOF) actuation. Patent disclosure received by OTC at UMD on 12 March 2008
- [30] King J K, Davis L M, Canfield B K, Sampson P C and Hofmeister W H 2009 Microfluidic device for the 3-D electrokinetic manipulation of single molecules *Frontiers in Optics, OSA Tech. Dig.* (CD) Optical Society of America, paper FWM4 <http://www.opticsinfobase.org/abstract.cfm?URI=FiO-2009-FWM4>
- [31] Pavani S R P, Thompson M A, Biteen J S, Lord S J, Liu N, Twieg R J, Piestun R and Moerner W E 2009 Three-dimensional, single-molecule fluorescence imaging beyond the diffraction limit by using a double-helix point spread function *Proc. Natl Acad. Sci.* **106** 2995–9
- [32] Pavani S R P and Piestun R 2008 Three dimensional tracking of fluorescent microparticles using a photon-limited double-helix response system *Opt. Express* **16** 22048–57
- [33] Jo B H, Van Lerberghe L M, Motsegood K M and Beebe D J 2000 Three-dimensional micro-channel fabrication in polydimethylsiloxane (PDMS) elastomer *J. Microelectromech. Syst.* **9** 76–81
- [34] Zhang M, Wu J, Wang L, Xiao K and Wen W 2010 A simple method for fabricating multi-layer PDMS structures for 3D microfluidic chips *Lab Chip* **10** 1199–203
- [35] Zhou T, Liu A L, He F Y and Xia X H 2006 Physicochemical and engineering aspects : time-dependent starting profile of velocity upon application of external electrical potential in electroosmotic driven microchannels *Colloids Surf. A* **277** 136–44
- [36] Yan D, Nguyen N T, Yang C and Huang X 2006 Visualizing the transient electroosmotic flow and measuring the zeta potential of microchannels with a micro-PIV technique *J. Chem. Phys.* **124** 021103–4
- [37] Gillespie D T 1996 The mathematics of Brownian motion and Johnson noise *Am. J. Phys.* **64** 225–40
- [38] Ropp C, Cummins Z, Probst R, Qin S, Fourkas J T, Shapiro B and Waks E 2010 Positioning and immobilization of individual quantum dots with nanoscale precision *Nano Lett.* **10** 4673–9
- [39] Hoshino A, Fujioka K, Oku T, Suga M, Sasaki Y F, Ohta T, Yasuhara M, Suzuki K and Yamamoto K 2004 Physicochemical properties and cellular toxicity of nanocrystal quantum dots depend on their surface modification *Nano Lett.* **4** 2163–9
- [40] Kalman R 1960 A new approach to linear filtering and prediction problems *Trans. ASME–J. Basic Eng.* **82** 35–45
- [41] Grover B R and Patrick Y C H 1996 *Introduction to Random Signals and Applied Kalman Filtering* 3rd edn (New York: Wiley)
- [42] Thompson R E, Larson D R and Webb W W 2002 Precise nanometer localization analysis for individual fluorescent probes *Biophys. J.* **82** 2775–83
- [43] Juette M F and Bewersdorf J 2010 Three-dimensional tracking of single fluorescent particles with submillisecond temporal resolution *Nano Lett.* **10** 4657–466
- [44] McMahan M D, Berglund A J, Carmichael P, McClelland J J and Liddle J A 2009 3D particle trajectories observed by orthogonal tracking microscopy *ACS Nano* **3** 609–14